# High-temperature semiconducting cubic phase of $BiFe_{0.7}Mn_{0.3}O_{3+\delta}$

Sverre M. Selbach,[1] Thomas Tybell,[2,3] Mari-Ann Einarsrud,[1] and Tor Grande[1,*]
[1]*Department of Materials Science and Engineering, Norwegian University of Science and Technology, 7491 Trondheim, Norway*
[2]*Department of Electronics and Telecommunications, Norwegian University of Science and Technology, 7491 Trondheim, Norway*
[3]*NTNU NanoLab, Norwegian University of Science and Technology, 7491 Trondheim, Norway*
(Received 3 March 2009; revised manuscript received 28 May 2009; published 22 June 2009)

$BiFe_{0.7}Mn_{0.3}O_{3+\delta}$ with space group $R3c$ is reported to go through two phase transformations, first to the orthorhombic paraelectric phase (*Pbnm*) and finally to cubic perovskite structure with space group $Pm\bar{3}m$. A discontinuity in volume and enthalpy shown by thermal analysis revealed that both transitions were first order. Electrical conductivity measurements demonstrated that the material remains semiconducting also in the high-temperature cubic state. The conductivity and the temperature of the two phase transitions were shown to be strongly influenced by the partial pressure of oxygen and a *p*-type semiconductivity was suggested. Finally, oxygen hyperstoichiometry ($\delta$) of $BiFe_{0.7}Mn_{0.3}O_{3+\delta}$ was demonstrated.

DOI: 10.1103/PhysRevB.79.214113 PACS number(s): 77.80.Bh, 72.80.−r

## I. INTRODUCTION

Multiferroic materials have recently been the subject of intense interest due to the technological potential of materials possessing both ferroelectric and magnetic ordering.[1,2] $BiFeO_3$ possesses simultaneous ferroelectric, antiferromagnetic, and ferroelastic ordering above room temperature[3] and is the most studied multiferroic material. At ambient conditions $BiFeO_3$ crystallizes in the polar, rhombohedral space group $R3c$ and high-quality bulk single crystals with a large polarization of 60 $\mu C/cm^2$ have been reported.[4,5] The ferroelectric $T_C$ at 820–830 °C and the antiferromagnetic $T_N$ at 370 °C are well established[4,6] but the nature of the paraelectric phase has been subject of discrepancies in recent literature. Palai *et al.*[7] reported a primitive orthorhombic phase above $T_C$ and a cubic phase at 925 °C just below the peritectic decomposition temperature $T_{per}$ of about 935 °C. An endothermic calorimetric peak at 930 °C was also noted by Haumont *et al.*[8] The paraelectric crystal structure was conclusively determined as $GdFeO_3$ like, belonging to the space group *Pbnm* by a high-temperature neutron diffraction study by Arnold *et al.*[9] and not the recently proposed $P2_1/m$, $I4/mcm$, or $R\bar{3}c$.[8,10,11] The transition $R3c \rightarrow Pbnm$ is first order from group theory,[12] consistent with nonzero $\Delta V_{trs}$ and $\Delta H_{trs}$.[7–9,11] The vicinity of the phase transition at 925 °C to the peritectic temperature has hampered structural studies of the cubic polymorph and several groups observed decomposition of $BiFeO_3$ before reaching this phase.[8–11] A metallic cubic polymorph obtained through a second-order transition at high temperature and high pressure was recently reported by Redfern *et al.*[13] However, a thorough understanding of the high-temperature phase is still lacking.

One possibility to study the cubic phase is to suppress the phase-transition temperatures by chemical substitution with Mn on the *B* site, thereby circumventing the difficulties of studying $BiFeO_3$ in close vicinity of the $T_{per}$. $BiFe_{0.7}Mn_{0.3}O_3$ is isostructural with $BiFeO_3$ but with a lower $T_C$ of 660 °C.[14] Here we report the two first-order phase transitions $R3c \leftrightarrow Pbnm \leftrightarrow Pm\bar{3}m$ in $BiFe_{0.7}Mn_{0.3}O_3$ and show that the *Pbnm* and $Pm\bar{3}m$ polymorphs are both *p*-type semiconductors.

## II. EXPERIMENT

$BiFe_{0.7}Mn_{0.3}O_3$ was prepared by solid-state reaction between dried $Bi_2O_3$ (Aldrich >99.9%), $Fe_2O_3$ (Sigma-Aldrich 99.98%), and $Mn_2O_3$ [prepared from Riedel-de-Haën $Mn(CH_3COO)_2 \cdot 4H_2O$ >99.5%]. Pellets of stoichiometric binary oxide mixtures were covered in sacrificial powder in order to eliminate possible evaporation of $Bi_2O_3$ and fired once for 10 min at 900 °C before quenching in air. Evidence for evaporation of $Bi_2O_3$ and deviation from the nominal composition could not be observed. Considerable deviation from a Bi:(Fe+Mn) ratio 1:1 is not in concordance with recent phase diagrams of the system $Bi_2O_3$-$Fe_2O_3$ showing that there is no intrinsic solid solubility in $BiFeO_3$.[7,8,15] We confirmed this also by the preparation of a series of $BiFeO_3$ samples with intentional deviation from a Bi:Fe ratio 1:1. These samples contained the expected secondary phases due to nonstoichiometry and no variation in lattice parameters of $BiFeO_3$ with nominal composition could be observed. The nominal Bi/(Fe+Mn) ratio close to unity was inferred for the phase pure materials.

The oxygen nonstoichiometry, $\delta$ in $BiFe_{0.7}Mn_{0.3}O_{3+\delta}$, was determined by thermogravimetry on fine-crushed powders annealed for 30 min at 850 °C in 5.0 $N_2$ and cooled to ambient at 400 °C $h^{-1}$. This material was assumed to be stoichiometric ($\delta$=0), corresponding to only $Mn^{3+}$. Materials reheated in air to 850 °C and cooled at 200 °C $h^{-1}$ and samples quenched in air from 900 °C were found to have $\delta = 0.06 \pm 0.005$ and $\delta = 0.03 \pm 0.005$, respectively.

Differential thermal analysis (DTA) was performed with a Netzsch STA 449 C Jupiter in synthetic air or 5.0 $N_2$ atmosphere with 10 °C $min^{-1}$ heating and cooling rates. Dilatometry was done in synthetic air with a Netzsch DIL 402 C dilatometer using 10 °C $min^{-1}$ heating and cooling rates.

X-ray diffraction (XRD) patterns were collected for 20°–96° $2\theta$ with a $\theta$-$2\theta$ Bruker AXS focus diffractometer with Cu K$\alpha$ radiation and a LynxEye position sensitive detector (PSD), a step size of 0.014° $2\theta$, 0.2 mm divergence slits, and a total data acquisition time of 15 h per pattern. High-temperature XRD was done in air with a $\theta$-$\theta$ Bruker AXS D8 Advance with Cu K$\alpha$ radiation, a mri Physikalische

 

Geräte GmbH high-temperature stage, and a VANTEC-1 PSD. The powder sample was supported by an alumina crucible. Temperature calibration was performed by high-temperature X-ray diffraction (HTXRD) of MgO using an *S*-type thermocouple and the uncertainty in temperature is estimated to be <15 °C. Patterns were collected from 30 to 920 °C from 20° to 60° $2\theta$ with 0.1 mm divergence slits, a step size of 0.016° $2\theta$, and a total acquisition time of 79 min per pattern. Rietveld refinements were carried out with the software TOPAS R (Bruker AXS) using the space group $R3c$ (161) in the hexagonal setting, $Pbnm$ (62) and $Pm\bar{3}m$ (221).

Four-point conductivity measurements up to 912 °C were carried out with heating and cooling rates of 5 °C $min^{-1}$ in synthetic air, $N_2$, and $O_2$ on ceramic bars of >93% of crystallographic density prepared by solid-state reaction. Bars polished to a cross-sectional area of 0.15 $cm^2$ were attached to platinum wires. Further details on the experimental setup can be found elsewhere.[16]

## III. RESULTS

High-temperature x-ray diffraction of $BiFe_{0.7}Mn_{0.3}O_{3+\delta}$ in air [Figs. 1(a) and 1(b)] identifies the phase-transition sequence as $R3c \leftrightarrow Pbnm \leftrightarrow Pm\bar{3}m$. The intermediate $Pbnm$ polymorph is evident from the super-reflections ( *), Fig. 1(a), and the triplet splitting of the pseudocubic (110) reflection, Fig. 1(b), as in $BiFeO_3$.[9] At 880 and 900 °C the absence of super-reflections and splitting of the $(110)_{cub}$ reflection (other than from K $\alpha_1$ and K $\alpha_2$) identifies this phase as the aristotype perovskite structure $Pm\bar{3}m$. This is supported by a significant reduction in the full width at half maximum of the Bragg reflections from 860 to 880 °C. Attempts to refine the patterns collected at 880 and 900 °C within the commonly found space groups $R3m$, $B2mm$, $P2mm$, and $P4mm$ resulted in cubic lattice parameters. The transition from $Pbnm$ to $Pm\bar{3}m$ occurs between 860 and 880 °C. At 920 °C the sample decomposed peritectically to a nonperovskite phase and a liquid phase envisaged by a curved base line (not shown). Lattice parameters in Fig. 1(c) for the $R3c$ and $Pbnm$ polymorphs of $BiFe_{0.7}Mn_{0.3}O_{3+\delta}$ behave qualitatively in line with earlier reports on $BiFeO_3$.[7–9,11,17] As shown in the inset of Fig. 1(c), the primitive unit-cell volume increases by 0.5% from 62.98 $Å^3$ (860 °C, $Pbnm$) to 63.30 $Å^3$ (880 °C, $Pm\bar{3}m$), indicating a first-order phase transition with $\Delta_{trs}V > 0$.

DTA of $BiFe_{0.7}Mn_{0.3}O_{3+\delta}$ materials with different oxygen nonstoichiometry ($\delta$), presented in Fig. 2(a), reveals two distinct and reversible thermal events labeled $T_C$ and $T_2$, which corresponds to the transitions $R3c \leftrightarrow Pbnm$ and $Pbnm \leftrightarrow Pm\bar{3}m$ (see Fig. 1). Two phase transitions below the peritectic decomposition temperature are qualitatively in concordance with DTA traces reported for $BiFeO_3$.[7,8] The transition $Pbnm \leftrightarrow Pm\bar{3}m$ occurs at 872–896 °C upon heating and cooling, and is clearly reversible. Thus, the cubic polymorph exists over a broader temperature interval below $T_{per}$ in $BiFe_{0.7}Mn_{0.3}O_{3+\delta}$ than in $BiFeO_3$, where $T_2$ is 925–930 °C.[7,8,13] The ferroelectric Curie temperature signi-

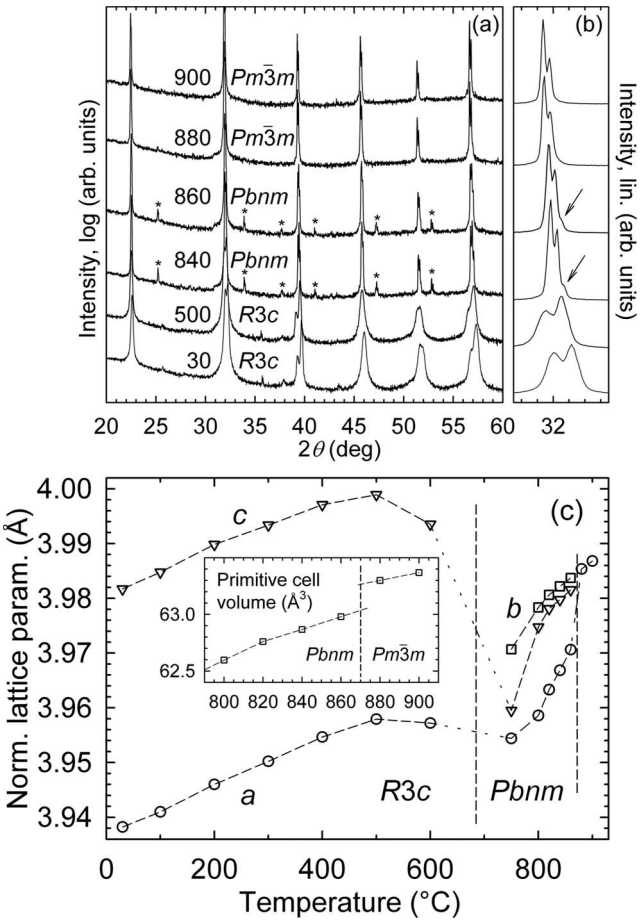


FIG. 1. (a) HTXRD patterns of $BiFe_{0.7}Mn_{0.3}O_{3+\delta}$ at selected temperatures (°C), plotted on a common log scale to envisage the low-intensity super-reflections arising from oxygen planes denoted by asterisks ( *). (b) Thermal evolution of the (110) pseudocubic reflection (linear scale); the arrows highlight the splitting into a triplet for the orthorhombic phase. (c) Refined lattice parameters of $BiFe_{0.7}Mn_{0.3}O_{3+\delta}$ for the $R3c$, $Pbnm$, and $Pm\bar{3}m$ phases. Inset: primitive unit-cell volume across the $Pbnm$ to $Pm\bar{3}m$ transition.

fied by endothermic peaks at 653–684 °C is in agreement with previous reports.[14] $\Delta_{trs}H_{T_C}$ is in the order of 1–2 kJ $mol^{-1}$, three to four times that of $\Delta_{trs}H_{T_2}$, showing that the transition at $T_2$ is also of first order. Normalized thermal expansion of a polycrystalline ceramic bar (>93% dense) shown in Fig. 2(b) confirms the first-order nature of the phase transitions at $T_C$ and $T_2$ as the volume is discontinuous across both. At $T_C$ the volume change is large and negative, $\Delta_{trs}V < 0$, as in $BiFeO_3$,[7–9,11] while at $T_2$ $\Delta_{trs}V > 0$, in line with the unit-cell volumes found from HTXRD [Fig 1(c)]. At elevated temperatures the effects of creep, sintering, and chemical expansion[18] are superimposed on the crystallographic thermal expansion, thus an absolute value of $\Delta_{trs}V$ could not be determined from dilatometry. The relative magnitudes of the thermal expansion anomalies at $T_C$ and $T_2$ correspond to the magnitude of the calorimetric signatures.

The influence of oxygen nonstoichiometry on the ambient temperature crystal structure is presented in Fig. 3. All three XRD patterns in Fig. 3(a) could be indexed with the space group $R3c$, e.g., the presence of the $(113)_{hex}$ super-reflection

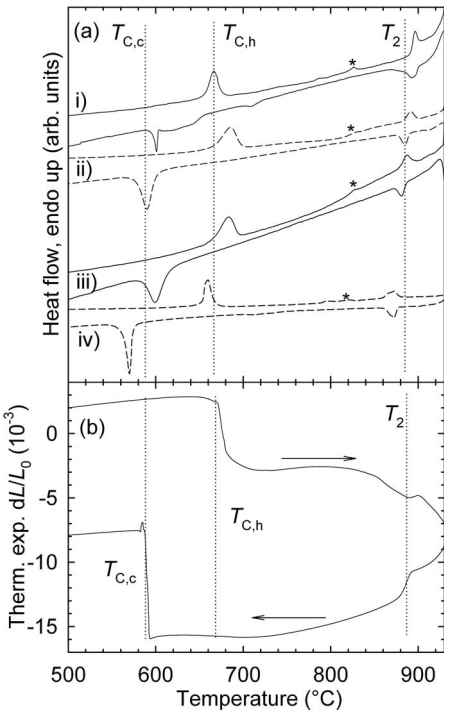


FIG. 2. (a) Differential thermal analysis of $BiFe_{0.7}Mn_{0.3}O_{3+\delta}$. (i) $N_2$ cooled from 850 °C ($\delta$=0) measured in $N_2$, (ii) quenched in air from 900 °C ($\delta=0.03\pm0.005$) measured in $N_2$ and (iii) air, and (iv) cooled from 850 °C in air ($\delta=0.06\pm0.005$) and measured in air. $T_{C,h}$ and $T_{C,c}$ denote the Curie temperature upon heating and cooling, respectively. Asterisks ( * ) denote minor peaks attributed to the $T_m$ of sillenite. (b) Dilatometric trace for an air-quenched $BiFe_{0.7}Mn_{0.3}O_{3+\delta}$ ceramic bar measured in air. Vertical dotted lines are guides for the eyes.

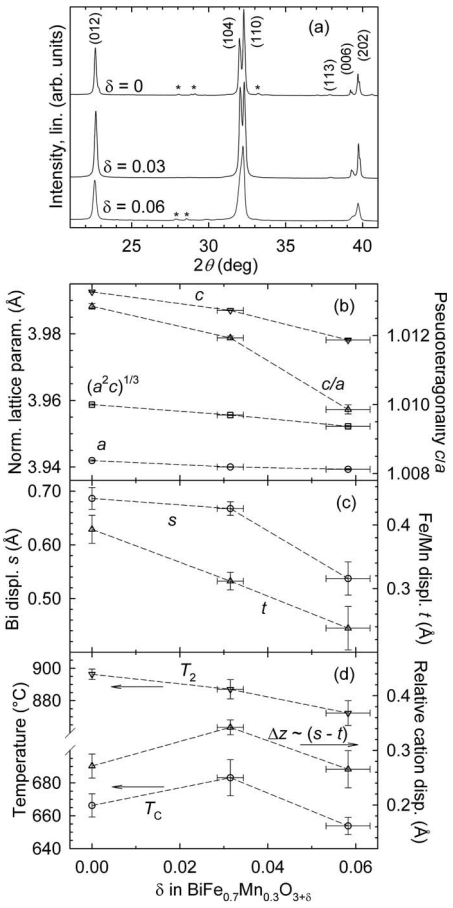


FIG. 3. (a) Room-temperature XRD patterns of $N_2$-cooled sample ($\delta$=0), air quenched ($\delta=0.03\pm0.005$), and air cooled ($\delta=0.06\pm0.005$) $BiFe_{0.7}Mn_{0.3}O_{3+\delta}$. Asterisks ( * ) denote reflections from traces of mullite and sillenite impurities. (b) Normalized lattice parameters, unit-cell volume, and unit-cell distortion $c/a$ as a function of oxygen hyperstoichiometry $\delta$. (c) Critical temperatures and polar cation displacements as a function of $\delta$. Corresponding values for $BiFeO_3$ from Ref. 3: $(a^2c)^{1/3}=3.964$ Å, $c/a=1.015$, and $(s-t)\sim\Delta z=0.405$ Å.

distinguishing $R3c$ from $R3m$.[19,20] Hence $BiFe_{0.7}Mn_{0.3}O_{3+\delta}$ remains isostructural with pure $BiFeO_3$ within the range of oxygen hyperstoichiometry investigated here. Refined lattice parameters and polar displacements[19] of Bi ($s$) and Fe/Mn ($t$) in Figs. 3(b) and 3(c) reveal that the crystal structure becomes less distorted (decreasing $c/a$) from the aristotype $Pm\bar{3}m$ with increasing $\delta$. The unit-cell volume $(a^2c)^{1/3}$ decreases linearly with $\delta$, in analogy with hyperstoichiometric $LaMnO_{3+\delta}$,[21] and chemical expansion in oxygen deficient perovskites upon reduction.[18] In perovskites, oxygen excess is compensated by cation vacancies; $Bi_{1-\delta/3}(Fe_{0.7}Mn_{0.3})_{1-\delta/3}O_3$. Excess oxygen in $BiFe_{0.7}Mn_{0.3}O_{3+\delta}$ must thus be charge compensated by the oxidation of $Mn^{3+}$ to $Mn^{4+}$, and the smaller ionic radius[22] of $Mn^{4+}$ (0.53 Å) than $Mn^{3+}$ (0.645 Å) explains the decreasing unit-cell volume. Correlations between phase-transition temperatures from DTA in Fig. 2(a) and crystallographic properties are shown in Fig. 3(d). The transition temperature of the transition $Pbnm\leftrightarrow Pm\bar{3}m$, $T_2$, decreases linearly with $\delta$. The ferroelectric $T_C$ follows the same trend as the relative cation displacements $(s-t)$, which is equivalent to the polar displacement $\Delta z$ of Fe/Mn along the polar $c$ axis with Bi fixed in *origo*.[23] This is in accordance with the relationship between $T_C$ and $\Delta z$ in ferroelectrics first pointed out by Abrahams *et al.*[24] Broader Bragg reflections [Fig. 3(a)] of the air-cooled sample ($\delta$=0.06) than for the quenched ($\delta$=0.03) reflect disorder or chemical inhomogenity introduced upon oxidation during cooling. The presence of detectable amounts of the commonly found secondary phases[25] sillenite ($Bi_{25}FeO_{39}$) and mullite ($Bi_2Fe_4O_9$) in the cooled samples, but not in the quenched, is explained by our previous analysis of the thermodynamic stability of $BiFeO_3$ and $BiFe_{0.7}Mn_{0.3}O_{3+\delta}$.[26]

Electrical conductivity anomalies are evident at both structural transitions, Fig. 4(a). A hysteresis in the conductivity is associated with the first transition $R3c\leftrightarrow Pbnm$, identified by vertical dashed lines. The higher conductivity of the paraelectric $Pbnm$ phase than the ferroelectric $R3c$ phase can be rationalized from the smaller unit-cell volume, as previously reported for $BiFeO_3$.[11] Anomalies associated with the transition $Pbnm\leftrightarrow Pm\bar{3}m$ are evident in the inset of Fig. 4(a). XRD of a crushed part of the polycrystalline sample bar after the measurement revealed no signs of decomposition.

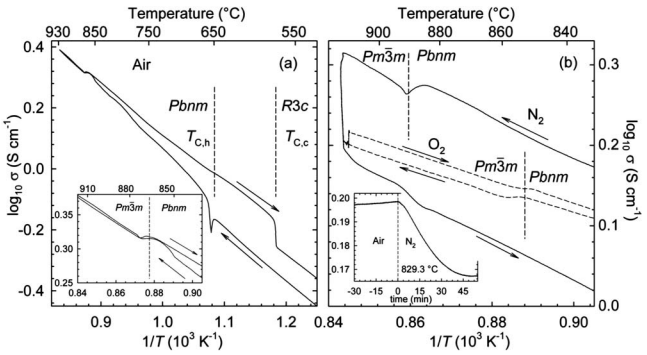


FIG. 4. (a) Conductivity trace for a $BiFe_{0.7}Mn_{0.3}O_{3+\delta}$ polycrystal measured in air. Inset: conductivity across the *Pbnm* to $Pm\bar{3}m$ transition. $T_{C,h}$ and $T_{C,c}$ denote the Curie temperature upon heating and cooling, respectively. (b) Conductivity traces across the *Pbnm* to $Pm\bar{3}m$ transition measured in $N_2$ (solid line) and $O_2$ (dashed line). Inset: isothermal conductivity relaxation during *in situ* change in atmosphere from air to $N_2$.

The influence of oxygen nonstoichiometry on the electrical conductivity was investigated on a fresh sample in $N_2$ and $O_2$ atmospheres. After heating in air for 30 min at 829 °C, switching to $N_2$ atmosphere was followed by a conductivity relaxation stabilizing after ~50 min [inset of Fig. 4(b)]. When the partial pressure of oxygen is reduced, excess oxygen in $BiFe_{0.7}Mn_{0.3}O_{3+\delta}$ is removed by shifting the point defect equilibrium,

$$\delta/2O_2 \rightleftarrows \delta O_O^x + 2\delta h^\bullet + \delta/3V_{Bi}''' + \delta/3V_{Fe,Mn}''', \qquad (1)$$

toward the left (Kröger-Vink notation). Here, $V_{Bi}'''$ and $V_{Fe,Mn}'''$ are vacancies at the Bi and Fe/Mn sublattices, respectively. Loss of excess oxygen is accompanied by removing positive holes $h^\bullet$. A lower conductivity in $N_2$ thus suggests that $BiFe_{0.7}Mn_{0.3}O_{3+\delta}$ is a *p*-type semiconductor. Holes can be regarded as $Mn^{3+}$ oxidized to $Mn^{4+}$; $Mn^{4+} \rightleftarrows Mn^{3+} + h^\bullet$, thus the ratio $Mn^{4+}:\delta$ is 2:1 and the fraction of $Mn^{3+}$ oxidized to $Mn^{4+}$ is $2\delta/0.3$. Since unsubstituted $BiFeO_{3-\delta}$ is stoichiometric within an uncertainty of $\delta < 0.01$,[27] oxygen nonstoichiometry is predominantly charge compensated by the valence of Mn in $BiFe_{0.7}Mn_{0.3}O_{3+\delta}$. An anomaly associated with the *Pbnm* to $Pm\bar{3}m$ transition can be seen at 886–891 °C [Fig. 4(b)], corresponding to the calorimetric peak at 896 °C of sample (iv) with $\delta=0$ in Fig. 2(a). During 15 min at 913 °C the conductivity decreased possibly due to further loss of excess oxygen. Cation diffusion is known to be slow in related perovskites at these temperatures[28] preventing equilibrium conditions in a ceramic sample bar on the time scale of the experiment. When heating in $O_2$ atmosphere a small decrease in conductivity associated with the *Pbnm* to $Pm\bar{3}m$ transition is observed at 855–859 °C, a lower temperature than the calorimetric peak at 872 °C for sample (iv) with $\delta=0.06$ in Fig. 2(a). When kept isothermally at 910 °C in $O_2$, the increasing conductivity supports a *p*-type semiconducting cubic phase.

## IV. DISCUSSION

A direct transition from *Pbnm* to $Pm\bar{3}m$ must be first order according to group theory,[12] in line with the results from DTA, dilatometry, and HTXRD. In agreement with previous reports on $BiFeO_3$, the lattice parameters increase faster with temperature in the *Pbnm* ($a^-a^-b^+$) phase than the *R3c* ($a^-a^-a^-$) and $Pm\bar{3}m$ ($a^0a^0a^0$) polymorphs (Glazer's notation[29]).[7–9] In the *R3c* phase the thermal expansion of the chemical bonds and decreasing octahedral tilts are partly counteracted by decreasing cation displacements.[9,17] The combination of straightening of bond angles and increasing bond lengths in the *Pbnm* phase explains the steeper rise in unit-cell volume with temperature.[30] A first-order transition from *Pbnm* to $Pm\bar{3}m$ must hence be accompanied by a positive $\Delta_{trs}V$. Negative or zero $\Delta_{trs}V$ can only be expected if a high-spin to low-spin transition occurs for the *B* cation, as found in high-pressure studies.[31] The observed positive $\Delta_{trs}V$ and the high temperature is not consistent with the possibility of a Mott transition[32] to a metallic cubic state and $BiFe_{0.7}Mn_{0.3}O_{3+\delta}$ is shown to be a *p*-type semiconductor for both the $Pm\bar{3}m$ and the *Pbnm* polymorphs in air, $N_2$, and $O_2$ atmospheres.

The fraction of $Mn^{4+}$ in $BiFe_{0.7}Mn_{0.3}O_{3+\delta}$ scales with $2\delta/0.3$ and since $Mn^{4+}(0.53\ \text{Å}) < Mn^{3+}(0.645\ \text{Å})$, the average Goldschmidt tolerance factor *t* increases toward unity with increasing $\delta$. Equivalently, the polyhedral volume ratio $V_A/V_B$ increases toward 5.0, which is the value in absence of octahedral tilting.[33] Hence, with increasing $\delta$ the cubic $Pm\bar{3}m$ ($a^0a^0a^0$) polymorph is stabilized relative to the orthorhombic *Pbnm* ($a^-a^-b^+$) phase, as shown here. Extrapolation of $T_2$ as a function of $\delta$ in Fig. 3(d) suggests that $\delta$ is close to the maximum limit of 0.15 in $O_2$ atmosphere at 840–910 °C. A correlation between phase-transition temperatures and oxygen hyperstoichiometry is also known from the related material $LaMnO_{3+\delta}$.[34] Smaller unit-cell volumes of $BiFe_{0.7}Mn_{0.3}O_{3+\delta}$ in air [inset of Fig. 1(c)] than $BiFeO_3$ (Ref. 9) in the *Pbnm* polymorph at equal temperatures follows naturally from the partial oxidation of Mn associated with oxygen hyperstoichiometry. Perovskites with $GdFeO_3$ structure usually transform from *Pbnm* to the centrosymmetric rhombohedral space structure $R\bar{3}c$ upon heating, e.g., $LaGaO_3$ (Ref. 35) but our data show no indications of an $R\bar{3}c$ precursor phase to the ideal perovskite structure $Pm\bar{3}m$.[36]

## V. CONCLUSION

In summary, $BiFe_{0.7}Mn_{0.3}O_{3+\delta}$ displays the phase-transition sequence $R3c \leftrightarrow Pbnm \leftrightarrow Pm\bar{3}m$. Both transitions are shown by calorimetry, dilatometry, and HTXRD to be discontinuous first order. The $Pbnm \leftrightarrow Pm\bar{3}m$ transition is accompanied by a discontinuous increase in unit-cell volume. Conductivity measurements in air, $N_2$, and $O_2$ identify the orthorhombic *Pbnm* and cubic $Pm\bar{3}m$ polymorphs as semiconductors, and the increasing conductivity with increasing partial pressure of $O_2$ suggest a *p*-type conductivity. The cubic polymorph is stabilized with increasing hyperstoichiometry $\delta$.

**ACKNOWLEDGMENTS**

Julian Tolchard and Guttorm Syvertsen at NTNU are acknowledged for assisting in HTXRD and conductivity measurements, respectively. This work was supported by the Norwegian University of Science and Technology and the Research Council of Norway (NANOMAT, Grants No. 158518/431, No. 140553/I30, and No. 162874/V00).

*Corresponding author; tor.grande@material.ntnu.no

[1] W. Eerenstein, N. D. Mathur, and J. F. Scott, Nature (London) **442**, 759 (2006).
[2] R. Ramesh and N. A. Spaldin, Nature Mater. **6**, 21 (2007).
[3] F. Kubel and H. Schmid, Acta Crystallogr. B **46**, 698 (1990).
[4] J. R. Teague, R. Gerson, and W. J. James, Solid State Commun. **8**, 1073 (1970).
[5] D. Lebeugle, D. Colson, A. Forget, M. Viret, P. Bonville, J. F. Marucco, and S. Fusil, Phys. Rev. B **76**, 024116 (2007).
[6] C. Michel, J. M. Moreau, G. D. Achenbach, R. Gerson, and W. J. James, Solid State Commun. **7**, 701 (1969).
[7] R. Palai, R. S. Katiyar, H. Schmid, P. Tissot, S. J. Clark, J. Robertson, S. A. T. Redfern, G. Catalan, and J. F. Scott, Phys. Rev. B **77**, 014110 (2008).
[8] R. Haumont, I. A. Kornev, S. Lisenkov, L. Bellaiche, J. Kreisel, and B. Dkhil, Phys. Rev. B **78**, 134108 (2008).
[9] D. C. Arnold, K. S. Knight, F. D. Morrison, and P. Lightfoot, Phys. Rev. Lett. **102**, 027602 (2009).
[10] I. A. Kornev, S. Lisenkov, R. Haumont, B. Dkhil, and L. Bellaiche, Phys. Rev. Lett. **99**, 227602 (2007).
[11] S. M. Selbach, T. Tybell, M.-A. Einarsrud, and T. Grande, Adv. Mater. **20**, 3692 (2008).
[12] C. J. Howard and H. T. Stokes, Acta Crystallogr. A **61**, 93 (2005).
[13] S. A. T. Redfern, J. Walsh, S. M. Clark, G. Catalan, and J. F. Scott, arXiv:0901.3748 (unpublished).
[14] J. R. Sahu and C. N. R. Rao, Solid State Sci. **9**, 950 (2007).
[15] A. Maître, M. François, and J. C. Gachon, J. Phase Equilib. Diffus. **25**, 59 (2004).
[16] I. Waernhus, P. E. Vullum, R. Holmestad, T. Grande, and K. Wiik, Solid State Ionics **176**, 2783 (2005) .
[17] A. Palewicz, R. Przenioslo, I. Sosnowska, and A. W. Hewat, Acta Crystallogr. B **63**, 537 (2007).
[18] S. B. Adler, J. Am. Ceram. Soc. **84**, 2117 (2001).
[19] H. D. Megaw and C. N. W. Darlington, Acta Crystallogr. A **31**, 161 (1975).
[20] A. M. Glazer, Acta Crystallogr. B **31**, 756 (1975).
[21] J. Töpfer and J. B. Goodenough, J. Solid State Chem. **130**, 117 (1997).
[22] R. D. Shannon, Acta Crystallogr. A **32**, 751 (1976).
[23] S. M. Selbach, T. Tybell, M.-A. Einarsrud, and T. Grande, Chem. Mater. **19**, 6478 (2007).
[24] S. C. Abrahams, S. K. Kurtz, and P. B. Jameson, Phys. Rev. **172**, 551 (1968).
[25] M. Valant, A.-K. Axelsson, and N. Alford, Chem. Mater. **19**, 5431 (2007).
[26] S. M. Selbach, M.-A. Einarsrud, and T. Grande, Chem. Mater. **21**, 169 (2009).
[27] M. Li and J. L. MacManus-Driscoll, Appl. Phys. Lett. **87**, 252510 (2005).
[28] M. Palcut, K. Wiik, and T. Grande, J. Phys. Chem. C **111**, 813 (2007).
[29] A. M. Glazer, Acta Crystallogr. B **28**, 3384 (1972).
[30] H. D. Megaw, Mater. Res. Bull. **6**, 1007 (1971).
[31] A. G. Gavriliuk, V. V. Struzhkin, I. S. Lyubutin, S. G. Ovchinnikov, M. Y. Hu, and P. Chow, Phys. Rev. B **77**, 155112 (2008).
[32] N. F. Mott, Rev. Mod. Phys. **40**, 677 (1968).
[33] N. W. Thomas, Acta Crystallogr. B **52**, 954 (1996).
[34] J. A. M. van Roosmalen, P. van Vlaanderen, E. H. P. Cordfunke, W. L. Ijdo, and D. J. W. Ijdo, J. Solid State Chem. **114**, 516 (1995).
[35] C. J. Howard and B. J. Kennedy, J. Phys.: Condens. Matter **11**, 3229 (1999).
[36] See EPAPS Document No. E-PRBMDO-79-075921 for (details on experiments, XRD results and conductivity measurements). For more information on EPAPS, see http://www.aip.org/pubservs/epaps.html.